Impact Assessment of Cloud Condensation Nuclei (CCN) Concentration on a Typhoon Evolution; A Numerical Case Study

Khan, M. T.[1, 2, 3], Y. Yin[3], A. Anjum[2], W. Yong[3]

Abstract

The typhoon Fanapi (14-23 Sept. 2010) is simulated for three different concentrations of cloud condensation nuclei (CCN) by using the Weather Research and Forecasting model (WRF). Sensitivity tests were carried out for varying aerosol concentrations, to determine the average and maximum response of microphysical processes of five different hydrometeors, minimum sea level pressure (MSLP), wind speed and radar reflectivity, to CCN. The clean case is ruminated as standard for comparison. MSLP increased by up to 7 hPa with higher concentration of CCN. The typhoon speed with higher CCN concentration remained faster, while surface wind speed remained higher for lower CCN simulation. Rainfall exhibits the momentous, spatial and temporal variability. The enhanced CCN concentration augmented rain / cloud droplet concentration and their mass mixing ratio. The concentration of graupel particles augmented with simulation time. The number concentration and mass mixing ratio of ice crystals were also observed on higher side with increased polluted cases, at mature stages. The increasing CCN reduces warm rain at early stage, responding into numerous snow particles, to grow by coagulations with cloud and rain drops at higher levels and stay longer in the atmosphere. It results in intensified precipitation at the later stage. Radar reflectivity also increased with higher CCN at initial and dissipating stages. The high CCN concentration delayed the typhoon growth by stirring up changes in hydrometeor properties, transforming the thermodynamic structure and hurricane diabetic heating distribution, and hence resulting into impact on typhoon intensity through comprehensive dynamical changes.

Key Words: Typhoon, concentration, CCN, microphysics, simulation.

Introduction

Typhoons are known for their mammoth power, and are always appended with torrential rainfall, storm surges, and tremendous winds. Its intensity is associated to the heat and moisture fluxes, and can consequently be verified by sea surface temperature (SST) and wind shear (Khain and Sutyrin 1983; Emanuel 2005). According to Intergovernmental Panel on Climate Change IPCC AR4 (2007), the intense tropical cyclone activity has increased in the post 1970's period and its future trends also indicates likely to increase during the 21st century. Wang et al. (2007) referred the South China Sea (SCS) as a significant area for the cyclone genesis. The frequencies of typhoon and tropical cyclone in the Northwest Pacific have been observed as 16 and 25.7 events per year, respectively (Neumann, 1993).

Aerosol particles, either from natural or anthropogenic locale (Penner et al. 2001; Zhang et al. 2004) have the ability to serve as cloud condensation nuclei (CCN) and likely influence the cloud microphysics, clouds development and time span, precipitation amount, albedo and electrification (Ramanathan et al., 2001). Several model based studies also revealed the drastic decrease of precipitation, with the increase of CCN concentration (Khain & Pokrovsky, 2004; Cui et al. 2006). The increase in aerosol enhances the cloud droplet number concentration Nd, and brings changes in cloud albedo (Penner et al. 2001).

The concentrations of cloud droplets and ice crystals correspond to the available CCN and ice nuclei (IN), which depend upon the characteristics of the local aerosols (Morrison et al., 2005). Therefore, variation in aerosol population directly impact on the cloud droplet number concentration, reduces drop size, and consequently results in increase the Liquid Water Content (LWC) in the atmosphere and cloud optical thickness (Twomey, 1974; Albrecht, 1989; Morrison et al., 2005). CCN influences the cloud drop number

[1] tahirdd@gmail.com
[2] Research and Development Division, Pakistan Meteorological Department, Pitrus Bukhari Road, Sector H-8/2, Islamabad, Pakistan.
[3] Nanjing University of Information Science & Technology (NUIST), Nanjing 210044, China

concentration, higher is its population; more cloud droplets will be formed. The redistribution of energy takes place due to enhanced CCN concentration and its allied changes. The modification in CCN concentration subsequently impacts temporal variation, auto-conversion process, efficiency and cloud-rain conversion. Naturally, the droplets of pure water in the clouds do not form by homogeneous nucleation. Instead, it is formed by heterogeneous process on the atmospheric aerosol particles. The liquid water contents increases with the height from the cloud base. It attains its peak values in the upper half of the clouds and then dwindles towards its top. Higher aerosol concentration domino effect is decrease in cloud droplet size; decelerate the collision process and lodging in atmosphere for a longer time period.

Various studies have been made to envision the impact of aerosol modification on the droplet concentration; however aerosol-ice interactions also encompass a profound impact on ice and mixed-phase clouds (DeMott et al., 1997; Lohmann 2002). CCN have an extensive impact on the rainfall instigation and clouds pattern. High number concentration of anthropogenic aerosols results in increase or decrease of rainfall, depending on their physical and chemical properties. It slows down the process of formation of rain drops by producing a large number of tiny cloud droplets (Gunn et al. 1957; Rosenfeld 1999) and It results in increased cloud top with enhanced LWC (Khain et al. 2005). During the past few decades, studies ascertained that CCN not only significantly result in changes in cloud microphysics but also have impact on cloud dynamics, discharge of latent heat and precipitation (Rosenfeld et al. 2008; Khain et al. 2009). It is observed that CCN rejuvenate the tropical convection by increase of vertical velocities and cloud top of the towering clouds (Khain and Pokrovsky 2004; Khain et al. 2005, 2009).

Simpson and Malkus (1964) anticipated that the additional latent heat, released by seeding the super cooled water, presented in the eyewall cloud, would produce a hydrostatic pressure drop that would modestly reduce the surface pressure gradient and as a consequence, the maximum wind speed decreases (Cotton et. al. 2007). The original hypothesis was subsequently modified by following a series of numerical hurricane simulations. Those numerical experiments suggested that application of the individual cloud dynamic seeding hypothesis to towering cumuli, near the outward of eyewall results into enhanced vertical development of towering cumuli. It causes the removal of low-level moisture from the boundary layer. The loss of moisture outward from the eyewall would starve the clouds for moisture in the eyewall region, causing a shift in the eyewall convection outward to greater radii and the storm should rotate slower and the winds diminish appreciably. A study on modification of Hurricane Katrina has been made by restraining the formation of warm rain in the superficial regions of the storm and hence concluded that the wind force reduced by up to 25 % on introduction of seeding particles (Rosenfeld et al. 2007).

Zhang et al. (2007) investigated the impact of Saharan dust (SAL), acting as CCN, on the tropical cyclone with variable CCN concentration and concluded that mounting CCN concentration between 1-5 km layer results in reduction of mean mass diameter and increase of the cloud droplet number concentration, during the entire simulation period, except the initial spin-up. Cotton et al., (2007) found the maximum decrease of 20m s^{-1} in the surface wind speed of the storm with increased CCN concentration. It motivated them to suggest that seeding of the tropical cyclone by CCN can be a viable mean of reducing its intensity.

The seeding with small hygroscopic particles, probably less than 0.1 μm in diameter, might result in significant reduction in storm intensity, with concomitant reductions in storm wind damage and storm surge damage (Cotton et al., 2007). Rosenfeld et al., (2008a) used the WRF model by using two nested grids to simulate the evolution of Hurricane Katrina and found that hurricane wind force area decreased by a half; while not changing much the peak winds at the smaller diameter of eyewall.

The Model and Experiments

The microphysical parameterization schemes become more sophisticated, in the current age, with the increasing computing power and are capable to calculate mass and mixing ratios of the different hydrometeors and can distinguish the size spectra with a distribution function. (Lin et al. 1983; Rutledge et al. 1984; Dudhia 1989; Walko et al. 1995; Reisner et al. 1998). The current refining of the bulk model scheme, are able to predict two moments number concentration, mass mixing ratio and hydrometeor size

spectra (Harrington et al. 1995; Meyers et al. 1992; Girard et al. 2001; Morrison et al. 2005). The aim behind meticulous treatment of the cloud droplet concentration and nucleation process in a numerical model is that, anthropogenic aerosol affects the clouds microphysical and radiative properties (Twomey 1977; Albrecht 1989).

This study is aimed to determine the impact of CCN variation on cloud physical processes in Typhoon Fanapi, 14-23 September 2010. The typhoon Fanapi hit Taiwan and Zhangzhou, China, has been simulated by using the Weather Research and Forecasting Model (WRF) coupled with the Morrison double moment microphysical scheme (Morrison et al. 2005) for three different CCN populations of clean or Marine case (100 cm-3), polluted or Continental case (1000 cm^{-3}) and very polluted case (2000 cm^{-3}). The CCN are presumed to be composed of ammonium sulfate (NH4)2SO4 and is based on the studies by Fitzgerald (1974) and Takeda et al. (1982) that chemical composition of CCN do not much change the expected size distribution of the cloud droplets. The clean case with CCN of 100 cm^{-3} is assumed as the base run for comparison with the other two cases.

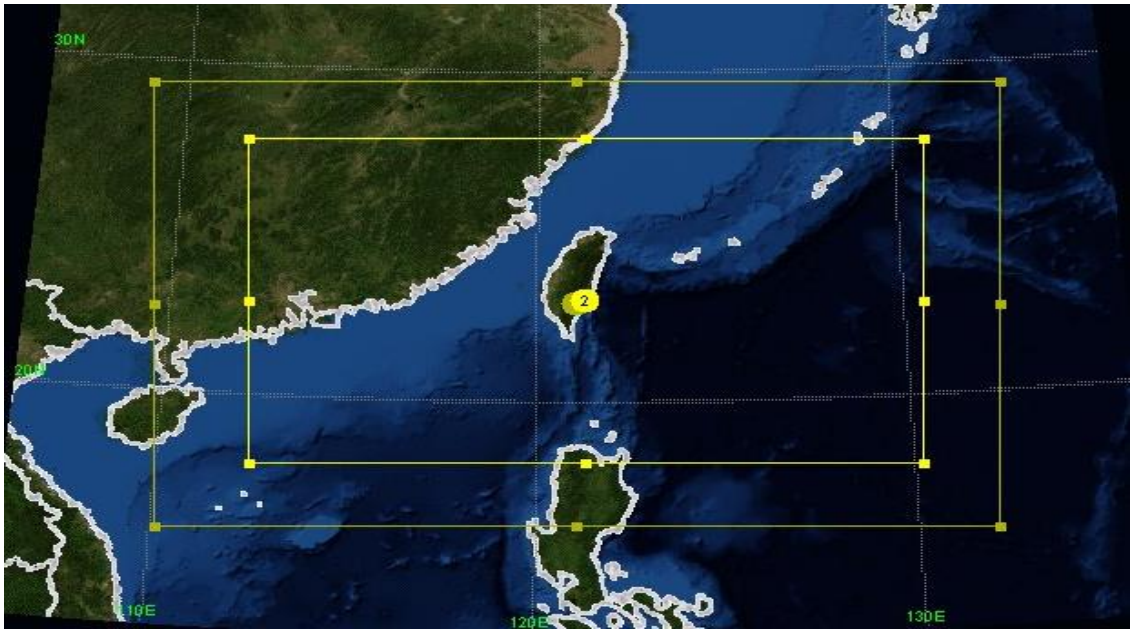

Figure 1: Nested domains selected for the typhoon Fanapi simulations

The NCEP GRIB-I format data has been used to initiate the simulation and was expanded for two nested domains (D-1 and D-2) with spatial resolution of 30 km and 10 km, between the latitude 16.1898°N – 29.5682°N and longitude 108.831°E – 133.696°E, (Figure 1 refers) while 19 vertical levels have been envisaged. The domain D-1 consist of 100, 64, 28 and D-2 with 238, 139, 28 grid boxes. The Lambert map projection is used in the model. The small time-split steps are used for acoustic and gravity wave models. Rapid Radiative Transfer Model (RRTM) Scheme for long wave and Dudhia scheme with a physical call of 30 minutes for short wave radiations are used in the model. Monin Obukhov scheme for surface layer, thermal diffusion scheme for land surface and YSU scheme with the physical call of 5 minutes are used in the model. Runge-Kutta and advection schemes along the horizontal and vertical dimensions are used in the model. The Arakawa C-grid is the grid staggering. The Morrison double moment bulk microphysical scheme used in this study predict the number concentration and mass mixing ratios of the five hydrometeors, that is, the cloud droplets, rain drops, ice crystals, snow, and graupel (Morrison et al., 2005). The microphysical parameterization and nested grid interaction have been tested (Vaid et al. 2013) and spatial distributions of large scale circulation, dynamical and thermodynamical fields were simulated reasonably well in the model. The size distribution function of cloud droplets and ice crystals, ϕ is given by the gamma function,

$$\phi(D) = N_0 D^{\mu} e^{-\lambda D} \quad \ldots (1)$$

Here D is particle diameter, N_0 the intercept, and λ the slop variable. $\mu = 1/\eta^2 - 1$ is the spectra shape parameter, λ the relative radius dispersion of size distribution as specified by Martin et al. (1994). In Morrison scheme, time evolution of number concentration *N* and mixing ratio *q* are calculated by grid scale convective detrainment, advection, turbulence diffusion and other microphysical processes based on the following equations:

$$\frac{\partial N}{\partial t} + \frac{1}{\rho}\nabla.[\rho u N] = \left(\frac{\partial N}{\partial t}\right)_{nuc} + \left(\frac{\partial N}{\partial t}\right)_{evap} + \left(\frac{\partial N}{\partial t}\right)_{auto} + \left(\frac{\partial N}{\partial t}\right)_{accr} + \left(\frac{\partial N}{\partial t}\right)_{accs} + \left(\frac{\partial N}{\partial t}\right)_{het} + \left(\frac{\partial N}{\partial t}\right)_{\hom} + \left(\frac{\partial N}{\partial t}\right)_{mlt} + \left(\frac{\partial N}{\partial t}\right)_{sed} + \left(\frac{\partial N}{\partial t}\right)_{\det} + D(N) \quad \ldots. (2)$$

$$\frac{\partial q}{\partial t} + \frac{1}{\rho}\nabla.[\rho u q] = \left(\frac{\partial q}{\partial t}\right)_{cond} + \left(\frac{\partial q}{\partial t}\right)_{evap} + \left(\frac{\partial q}{\partial t}\right)_{auto} + \left(\frac{\partial q}{\partial t}\right)_{accr} + \left(\frac{\partial q}{\partial t}\right)_{accs} + \left(\frac{\partial q}{\partial t}\right)_{het} + \left(\frac{\partial q}{\partial t}\right)_{\hom} + \left(\frac{\partial q}{\partial t}\right)_{mlt} + \left(\frac{\partial q}{\partial t}\right)_{sed} + \left(\frac{\partial q}{\partial t}\right)_{\det} + D(q) \quad \ldots. (3)$$

Here, *t* represents time, ρ the density of air, *u* the three dimensional wind vector and *D* as the operator for turbulent diffusion. The *D(N)* and *D(q)* given in the above two equations are the grid average microphysical source/sink for number concentration *N* and mixing ratio *q*. The right-hand-side terms give the activation of CCN condensation/deposition on ice crystal; sublimation and evaporation, auto conversion of cloud droplets and ice crystals to form rain or snow, accumulation of cloud droplets and ice crystals to form snow, heterogeneous freezing to form ice, homogeneous freezing of tiny drops, sedimentation melting and convective detrainment.

Results and Discussions

The Japan Meteorological Administration (JMA) reported late on 14th September 2010 that a depression is formed SE of Taiwan. On next day it converted into Typhoon 'Fanapi' and lasted until 0000 GMT of 23rd September. The WRF simulations outcomes for varying CCN have been analyzed for five different hydrometeors. The experimental results are as below.

Response of Mean Sea Level Pressure to Changes in CCN

The Mean Sea Level Pressure (MSLP) during the initial development stages of all the three simulated cases, as shown in Figure 2, remained unchanged. However, after 0600 GMT, on 16th September the typhoon was originally reported to change its intensity to Cat-I typhoon by JMA. The differences became highest, when it made its first landfall over Taiwan. The pressure increased linearly and the typhoon became weak for all the three cases of CCN. The typhoon with very-polluted atmosphere weakens more rapidly than the other two cases. Due to availability of sufficient moisture and decrease in pressure, it started strengthening again. It has been observed that typhoon with low CCN concentration is stronger than higher CCN cases. The difference of 7 hPa in MSLP between the clean and very-polluted cases has been noted at this stage. It is observed that typhoon simulated with polluted and very polluted background moved faster than the clean case, and can be seen in Figure 1 at points A, B, C and D respectively.

The typhoon track analysis (Figure 2) shows a significant spatial variability during its initial developing stages. In comparison to the original track, an equator ward shift of the typhoon is observed after its

first landfall over Taiwan. However, no significant change has been noticed during its developing stages over the sea.

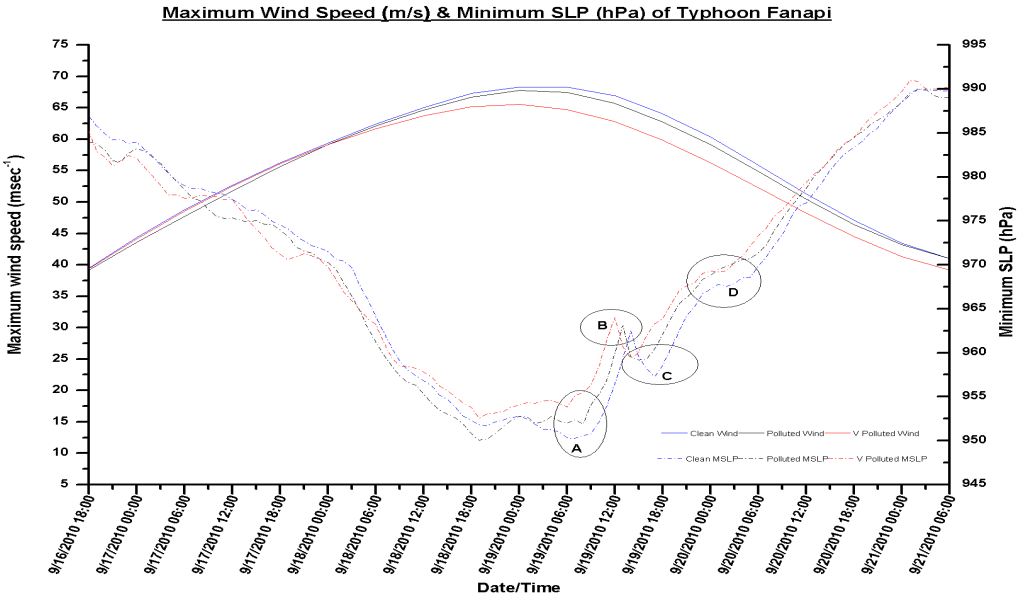

Figure 2: Temporal evolution of maximum wind speed and minimum sea level Pressure (MSLP) of typhoon Fanapi.

Response of Maximum Wind Speed to Changes in CCN

The maximum wind speed of the typhoon Fanapi was analogous, during the initial development stages, for all the three simulated cases. The major differences occurred at its mature stage (Figure 4) and at the time of its landfall over Taiwan (Figure 3). The wind speed in the clean case remained higher than the polluted and very-polluted cases and the results are substantial with Zhang et al. (2007). It was concluded that the spiral rain bands divert enthalpy from the core area of typhoon and hence result in diminishing of the storm. Similar results were also produced by Cotton et al. (2007). It can motivate to the seeding of typhoons, with small hygroscopic aerosols, could be a viable mean of reducing the typhoon intensity.

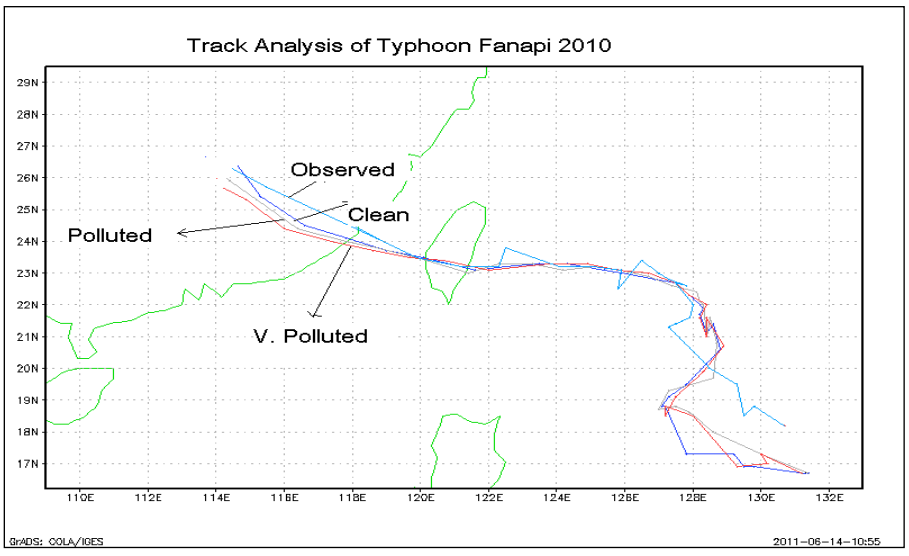

Figure 3: Comparison of the tracks of original and simulated cases of typhoon Fanapi

Precipitation Response to Changes in CCN

The cumulative rainfall regimes of three simulated cases, illustrate considerable temporal and spatial variability (Figure 4). The rain intensity started changing for the three variable concentrations of CCN, after 20:00 GMT, on 16th September and increased with typhoon development. The first peak in the rain intensity was observed on 18th September between 12:00 to 18:00 GMT as illustrated in Figure 4. The rainfall intensity in very-polluted case remained remarkably lower than the clean case. The second peak of was noted at the first landfall of the typhoon over Taiwan on 19th September, between 10:00–1800 GMT when it was originally of Cat-IV intensity. It weakens rapidly due to detachment to its energy source from the base. The precipitation intensity with the very-polluted background also indicated the decreasing trend, but no significant change is observed in clean and polluted cases.

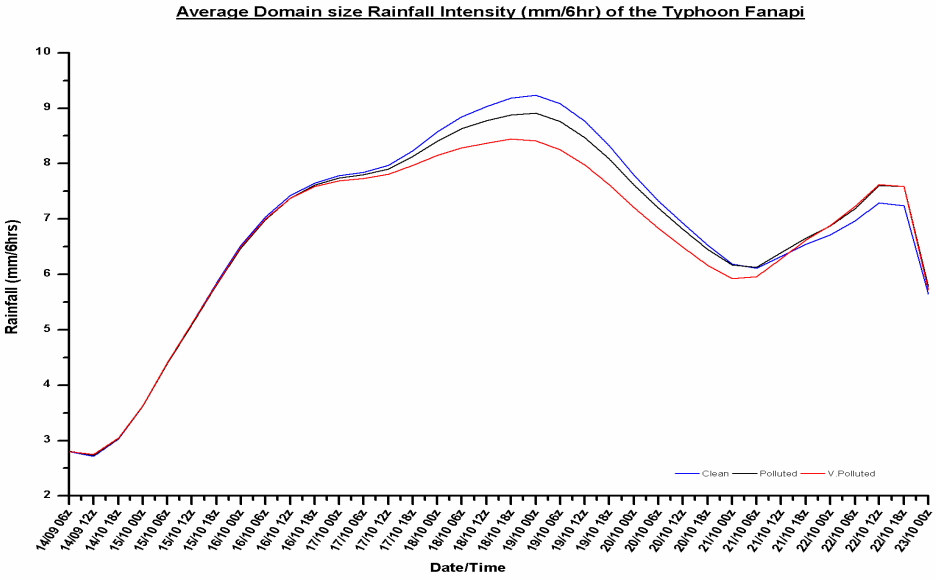

Figure 4: Temporal evolution of average domain size rainfall intensity of typhoon Fanapi.

Figure 4 indicates that in the afternoon of 19th September, the tropical cyclone developed again to Cat-I typhoon over SCS, and rain intensity also started sneaking up. The similar trend was perceived at 20:00 GMT on 19th September, with decreasing rain intensity from clean to polluted and very-polluted cases. The rainfall intensity reflected the non-monotonic reactions to increasing CCN; however, it is not well marked. The enhanced CCN concentration produced numerous small droplets and caused the reduction in rain quantity (Figure 5). In order to evaluate the impact of varying CCN concentration, it is required to investigate the hydrometeor physical properties beside the surface rainfall analysis.

Response of the Cloud Properties to Changes in CCN

The average cloud droplet concentration varies for all the three different aerosol populations. Figure 5 reveals the temporal variation of cloud droplets number concentration with the increasing CCN. It is observed that CCN activation occurred in a greater air volume, except the first 18 hours of initialization. The activated CCN determines the cloud droplet concentration generated through heterogeneous nucleation. Its concentration is noticed higher during the typhoon first landfall over Taiwan. The average mixing ratio is also in-association with cloud droplet number concentration. An increase in concentration was of 50 – 275 ($No*10^6$ /kg) for polluted and 75 – 435($No*10^6$ /kg) for very-polluted cases as compare to clean case, during the initial 36 hour. However, it is inconsistent during the developing stage of the typhoon. Significant variation is observed at first landfall and relics consistent to the end. The maximum cloud droplet concentration and mixing ratio also trail the similar tendency. It follows the theory of Hobbs et al. (1970) that increase of CCN causes the enrichment of cloud droplet population and decrease in its average size. As larger droplets are good collectors in warm clouds, and

can produce raindrops. The rain fall in the clean atmosphere is higher due to presence of less CCN; larger cloud droplet size and higher water accrual on them.

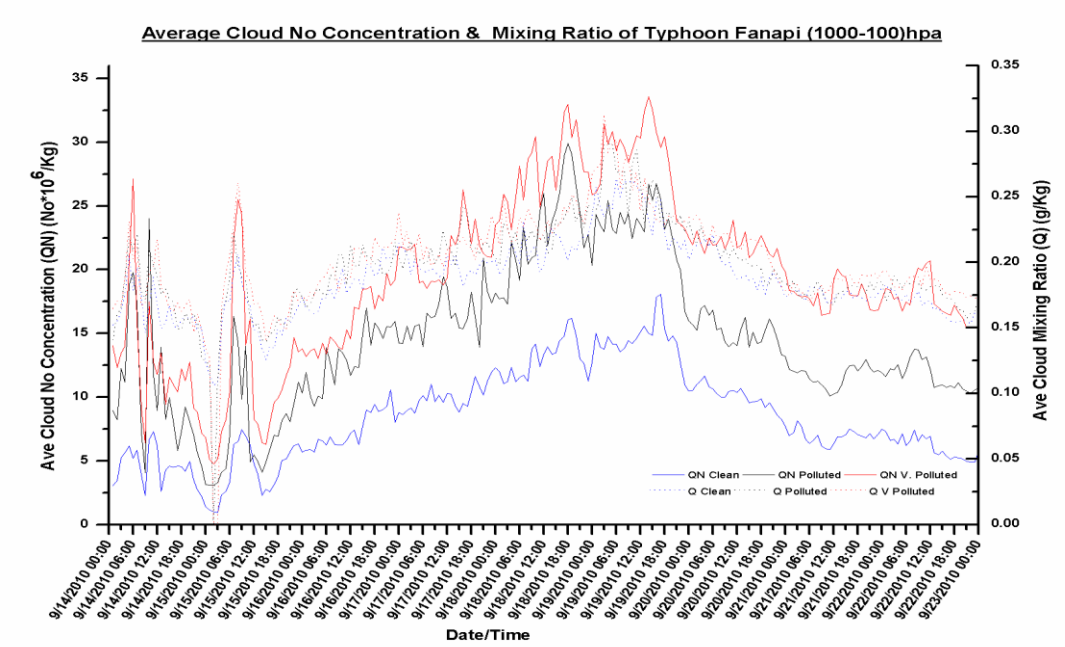

Figure 5: Temporal variation of average cloud number concentration and cloud mixing ratio of typhoon Fanapi.

To examine the changes in cloud droplet population and mixing ratio along the different pressure levels, vertical profiles for the 1st landfall of typhoon over Taiwan and 2nd landfall over ML China were plotted, which showed the monotonically increasing trend of droplet number concentration and mixing ratio with height for the increasing CCN. The cloud droplet number concentration for the very-polluted typhoon remained highest between the levels 950-350 hPa during both the landfalls. However, it was observed on the higher side during the first landfall over Taiwan than the second landfall over ML China. The mixing ratio, also remained higher for the very-polluted case than the polluted and clean cases, respectively, between the levels 900-800 hPa and 450-300 hPa over Taiwan. During the 2nd landfall, the mixing ratio for the very-polluted case remained higher between the levels 950- 500 hPa.

Response of Raindrops to Changes in CCN

Raindrops are formed by coagulation of cloud droplets. The average raindrop size lies between 0.1-5 mm and can be up to 8 mm in an exceptional case. The emergence of big raindrop indicates the strong updraft and turbulence. The larger raindrops move down, accumulating the small droplets on their path and expanding their volumes. Falling raindrops encounter air resistance or a frictional force that depends on their surface areas and sizes. The gravitational and frictional forces, finally, balance each other and raindrop falls at a constant speed depending on its size and orientation.

In this study, number concentration of the raindrops in the polluted and very- polluted background are observed lower than the clean case, as illustrated in Figure 6. It corroborates Rosenfeld (2000) that the raindrops in the polluted area are significantly smaller in size than those found over the clean area, i.e. less than 14µm (threshold value to form precipitation) in radius compared to 25µm. It also proves that cloud droplets formed in the clean background are highly potential to form precipitation than in the polluted backgrounds.

Figure 6 exhibits the trend of the average rain water mixing ratio at the early stages. It attained two peak values, indicating the increase in instability, in response to increasing CCN number concentration. It is noticed that rainwater mixing ratio in the clean case remain higher than polluted cases, imitating

higher instability. However, increasing CCN concentration delays the rain formation and reduces the time duration before freezing.

It is evident from above discussion that the growth of raindrop number concentration and rain water content changed with time evolution. Higher CCN number concentration led to smaller raindrops, reduced collision–coalescence and less rainout. It leads to greater convection and warming of upper atmosphere. Water is lifted above the freezing level. Raindrop number concentration is decreased by 10-30 % in the polluted case, and 15-37 % in very-polluted case. The maximum rain water mixing ratio trails the similar inclination and remained higher in clean case at the mature stage than the other two cases. It indicates that the raindrop size would be larger in the clean case, resulting into high precipitable amount.

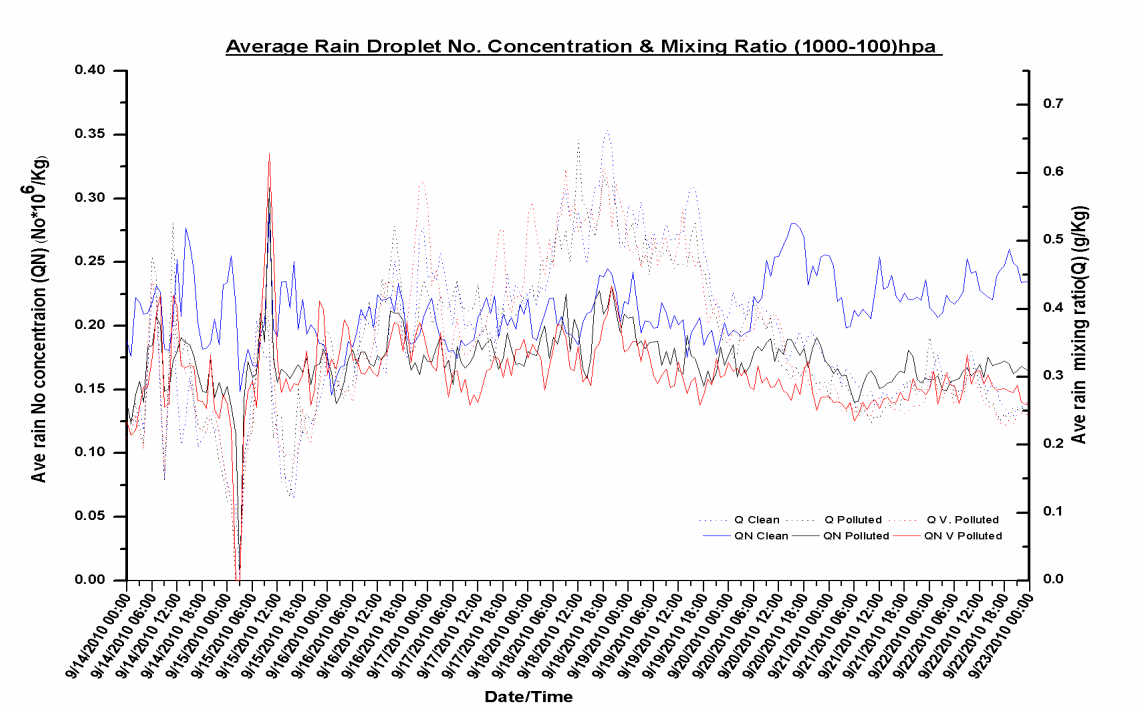

Figure 6: Temporal evolution of Average raindrop number concentration and rain water mixing ratio.

The vertical profiles for raindrop number concentration and mixing ratio have been drawn to evaluate the changes along different pressure levels. It is noted that rain droplet concentration, in the polluted and very-polluted cases remained inferior during both the landfalls at the lower and upper levels. However it was observed higher in the polluted case, between the levels 700 and 500 hPa. The rain water mixing ratio remained higher for the clean case than the polluted and very-polluted cases between the levels 900-850 hPa and 550-350 hPa. It remained higher in very-polluted case, at the middle level.

Response of Graupel to Changes in CCN

Graupel is formed by strong convective activity within a storm. At lower levels the particles collide and aggregate with the frequently available smaller particles. In the storm anvil, aggregation of the graupel is the main development pathway. The average number concentration of graupel particles in this case, initially highly reacted with the CCN and increases monotonically with the increase of CCN as in Figure 7. Analogous tendency was observed during the typhoon's first landfall over Taiwan and at mature stage. In the clean case the concentration of graupel particles started increasing as typhoon attained its mature stage and remained higher than the polluted and very-polluted cases. The average mixing ratio also followed the similar trend and remained about 0.6 g kg^{-1} during the initial stage, and between 0.2 - 0.7 g kg^{-1} during its mature stage. The mixing ratio was recorded highest as 0.71g kg^{-1} at

0300 GMT on 18th September for clean case. The average graupel mixing ratio for both the polluted atmosphere became lower than the clean case at the mature stage.

The maximum graupel number concentration is observed higher for both the polluted cases at the initial developing stages of the typhoon. The situation prevailed till the mature stage however; it befalls higher in favor of clean simulation during the dissipating stages. Graupel number concentration increased by 220 % and 255 %, respectively, for polluted and very-polluted cases than the base run clean case and decreased linearly towards the dissipating stages.

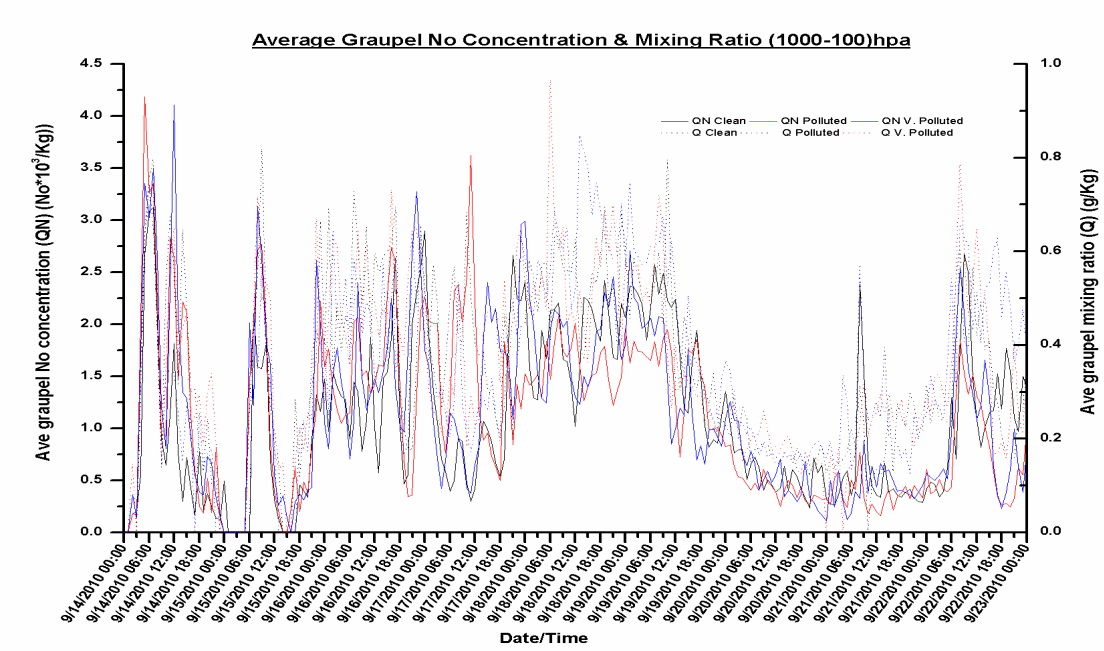

Figure 7: Temporal evolution of the average graupel number concentration and mixing ratio of typhoon Fanapi

The maximum graupel mixing ratio also followed the similar trajectory at the early stages. The situation starts changing on 18th September at 08:00 GMT, when the typhoon originally was of Cat-IV type and turned higher for clean simulation than the polluted cases. The maximum graupel mixing ratio followed the similar projections during the mature stage of the typhoon. This illustrates the idea that temperature rapidly falls in the vertical cross-section of the clean case. It is noted that number concentrations of graupel increased by 90 % and 165 %, during the early stage and decreased to -10 % during the mature stage. It has shown the positive anomaly towards the end of simulation. From above discussion, it is apparent that the graupel size in the polluted and very-polluted cases is smaller due to CCN abundance. Hence their collision and coagulation efficiencies are also diminutive. However, higher graupel concentration is observed at the diminishing stage in clean case, as its radius is large enough and is easily frozen into graupel.

The vertical profiles of the average graupel concentration remained higher in clean case between the levels 500-350 hPa. The average graupel mixing ratio also followed the similar pattern during the 1st landfall and remained higher at all levels above 600 hPa for the clean case.

Response of Ice Properties to Changes in CCN

The increasing CCN in both the polluted cases resulted in reduction of warm rain. It produces numerous tiny cloud droplets that are less efficient to initiate the collision and coalescence processes to produce rainfall. The super cooled droplets are carried up by the convergence to the layers cold enough to form ice particles, yielding numerous ice crystals that are ultimately lifted to the typhoon anvil. Large ice particles produced in the clean case had large terminal velocity, resulting into start of cold rain processes

and heavy precipitation rate. In the developing clouds the size of the particles grew up by riming. It is evident from Figure 8 that the number concentration of ice particles is higher at the initial developing stage of the typhoon. It decreased by 2-15 % in both the high CCN concentration cases at the initial stage. However, it remained higher at the mature stage in polluted and very-polluted cases. The super cooled water droplets or ice particles are found in the regions of strong updraft. The high concentration of CCN enhanced the amount of super cooled water droplets as well as ice content. Hence during the later stage of the typhoon, the updraft was strong and the ice particle number concentration increased.

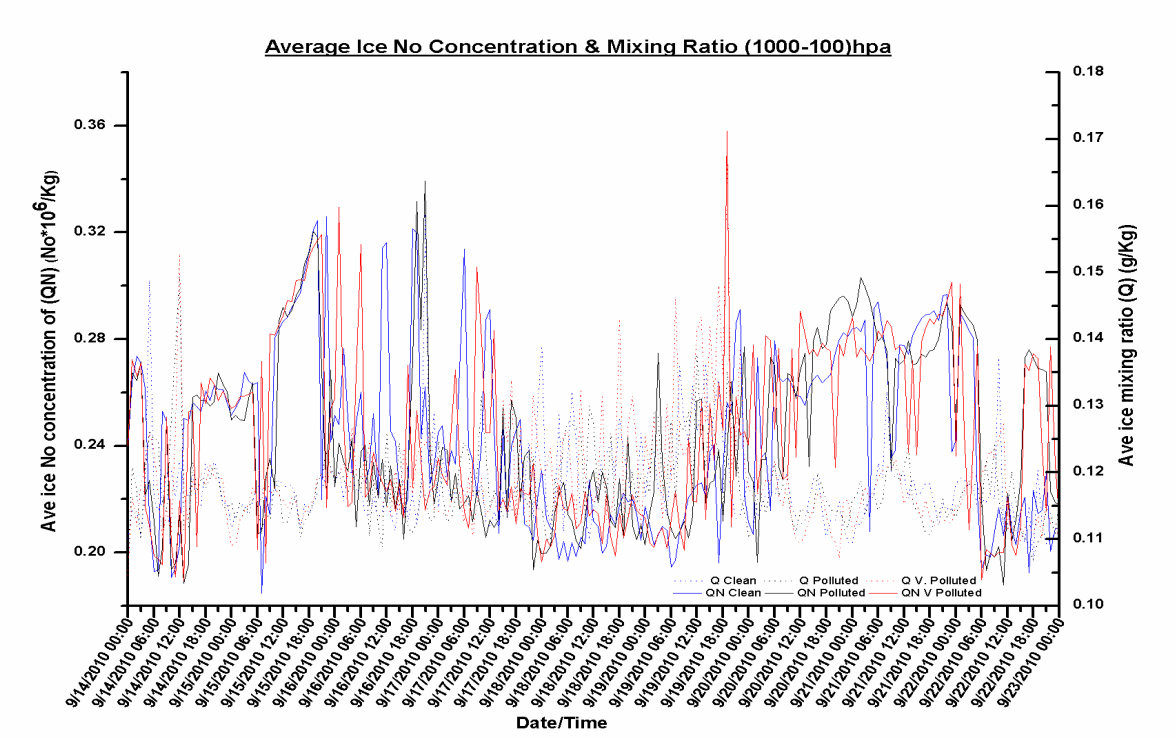

Figure 8: Temporal evolution of the average Ice number concentration and mixing ratio of typhoon Fanapi

The average ice mixing ratio also followed the similar trend. It remained higher in clean case during the initial developing stage. However, it surpassed in the very- polluted case at the later stage of simulation. It attains its peak value at 20:00 GMT of the 20th September while the typhoon was making its second landfall and decreased towards the dissipating stage. The major increase in maximum ice particle concentration and mixing ratio are observed during the period of September 18th at 08:00 GMT to 20th September 20:00 GMT. The peak values of 5-40 % for the polluted case are attained at 12:00 GMT on 19th September. In the very-polluted case, it was 25 % above than the clean case during the initial stage and remained 130 % above clean case, at 18:00 GMT of the same day.

The above results are in agreement with the intuition by Khain (2009) that increase in small CCN resulted in reduced droplet size and amplification of the population. It responds in deceleration of the collision and coalescence, rain drop formation and impediment in initiation of warm rain processes. Consequently, the small cloud droplets ascend in the updraft and grow by condensation process. This instigates the abundance of super cooled water droplets at higher levels and intensification of riming. These processes (diffusion drop growth and riming) results in release of extra latent heat, leading to enhancement of cloud updraft and cloud top height.

The vertical profiles of the ice particles reflected its higher concentration at the lower and middle levels, for the clean case, however, mixed trend was observed at levels above 300 hPa. The ice mixing ratio remained least, in the clean case, up to 250 hPa, and showed the mixed trend thereafter.

Response of Snow Properties to Changes in CCN

The infiltration of large quantity of small droplets above the freezing level results in development of large amount of snow and graupel in the periphery of the tropical cyclone (Khain et. al. 2009). The ice particles with diameter ≤ 150 μm are known as crystal whereas the bigger particles are referred to as snow particles. Aerosol induced in the typhoon increases the super cooled liquid water content and results in the conditions obsequious for the formation of graupel and ice particles.

Figure 9 indicates that average number concentration of snow particles in the polluted and very-polluted cases remains higher than the clean case. It rapidly grew up at initial stage of the typhoon and is related to the ice particles concentration. It decreased consistently with the developing stage of typhoon. A sharp increase in snow number concentration was observed as typhoon made it landfall over Taiwan. The highest increase was observed in the very-polluted case. It attained its second peak value on 20th September at 18:00 GMT and decreased monotonically towards the retreating stages.

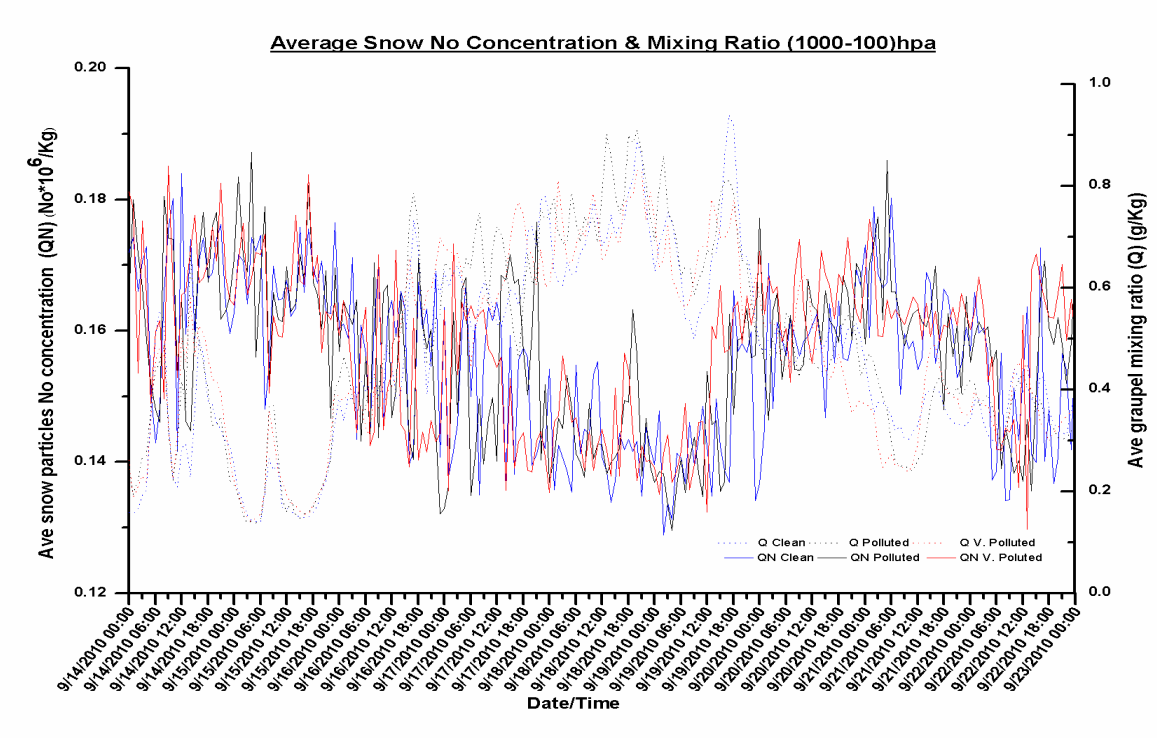

Figure 9: Temporal evolution of average snow number concentration and mixing ratio of typhoon Fanapi

The average snow mixing ratio increased by 10-65 % for high CCN cases, till the mature stage of typhoon, however, it decreased towards the diminishing phases. A small increase is observed in maximum snow particle number concentration at the initial stage followed by a mixed trend that continued up to 1600 GMT of 18th September. The maximum snow particles number concentration attained the 2nd peak value at this stage for the very-polluted case. It was observed highest when the typhoon was inland over Taiwan. The polluted case revealed a wave like trend by attaining two peaks and two troughs.

The maximum snow mixing ratio has shown a mixed trend during the early developing stage and got 1st peak value for the clean case in the afternoon of September 16th. The flagrant increase was observed for clean case on 16th and 22nd September 2010 with the peak values of 7.3 g kg^{-1} and 6.7 g kg^{-1}, respectively. However, it generally exhibits the increasing trend for both polluted cases in analogy to the clean case. The vertical profiles of snow number concentration and snow mixing ratio exhibits the increasing trend for the polluted and very-polluted cases in comparison to the clean case, along the different pressure levels.

Response of RADAR Reflectivity to the Changes in CCN

The reflectivity factor (Z) of RADAR is calculated from the number of drops in a unit volume of air and the sixth power of diameter of drops. The reflectivity depends upon the hydrometeor type (rain, snow and hail), size and their number concentrations. The large number of small hydrometeors reflects the same as one big hydrometeor. dBZ illustrates echo intensity and measures the strength of the weather activity. Radar reflectivity for both the polluted cases remained higher than the clean case, at the initial stages. The increasing CCN concentration resulted into numerous tiny cloud droplets leads to high reflectivity for the polluted and very-polluted cases as in Figure 10. The 6-7 % increase is observed during initial and dissipating stages of the typhoon. The reflectivity changed with the increasing CCN meditation.

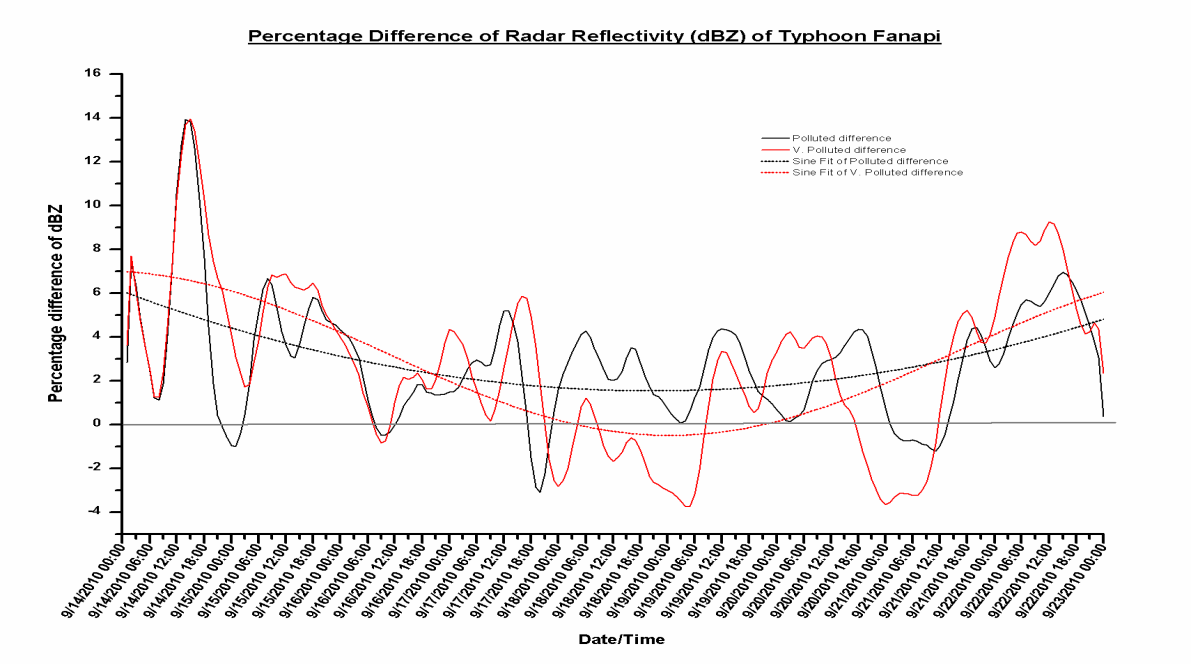

Figure 10: Temporal evolution of (Percentage) difference of average radar reflectivity (dBZ).

Conclusions

The numerical simulation of typhoon Fanapi was performed for three different concentrations of CCN. WRF model coupled with Morrison double moment microphysical scheme was used to investigate the impact of varying CCN on five distinct hydrometeors and their microphysical properties. The typhoon was observed as strongest with clean background atmosphere and lowest MSLP. The pressure difference of 7 hPa is observed between clean and very-polluted cases at the mature stage. The typhoon with both the polluted backgrounds moved faster than the clean case. The maximum surface wind speed corresponds to MSLP. The spatial and temporal variability in the rainfall has been observed. The rain-band became narrower with increasing CCN population over the ocean. The rain processes delayed for the higher aerosol concentration and exhibit the decreasing trend with increase in CCN concentration. The cloud droplet concentration significantly increased leading to reduction of the precipitable raindrop formation. The aerosol addition subsequently reduced the efficiency of auto conversion process from cloud to rain. The cloud droplet and rain mixing ratio also revealed the linear increasing trend to increasing CCN concentration. The mixing ratio and concentration of graupel also followed the similar trend at initial stages, however, a linearly decreased trend toward the dissipating stages of the typhoon. The ice particle concentration gradually increased with the typhoon development for higher polluted cases. The highest ice mixing ratio was recorded at mature stage, while it reflected the mixed trend at low pressure levels above.

The higher number concentration of snow particles are noticed for clean case at early developing stages and reaches to peak value at mature stages and upon typhoon landfall. The vertical profile of the snow mixing ratio increased as a function of time with the higher aerosol concentrations. The RADAR reflectivity (dBZ) also remained higher for polluted and very-polluted cases and exhibits the increasing trend.

References

Albrecht, B. A., 1989: Aerosols, cloud microphysics, and fractional cloudiness. Science, 245, 1227-1230.

Alley, R. B., et al., 2007: A report of Working Group-I of IPCC on Climate Change 2007: Summary for Policymakers, IPCC, AR-4, (2007), p-15.

Cotton, W. R., H. Zhang, G. M. McFarquhar, and S. M. Saleeby, 2007: Should we consider polluting hurricanes to reduce their intensity. J. Wea. Mod, 39, 70-73.

Cui, Z., K. S. Carslaw, Y. Yin, and S. Davies, 2006: A numerical study of aerosol effects on the dynamics and microphysics of a deep convective cloud in a continental environment. Journal of Geophysical Research: Atmospheres (1984–2012), 111.

DeMott, P. J., D. C. Rogers, and S. M. Kreidenweis, 1997: The susceptibility of ice formation in upper tropospheric clouds to insoluble aerosol components. Journal of Geophysical Research, 102, 19575-19519,19584.

Dudhia, J., 1989: Numerical study of convection observed during the winter monsoon experiment using a mesoscale two-dimensional model. Journal of the Atmospheric Sciences, 46, 3077-3107.

Fitzgerald, J. W., 1974: Effect of Aerosol Composition on Cloud Droplet Size Distribution: A Numerical Study. Journal of Atmospheric Sciences, 31, 1358-1367.

Girard, E., and J. A. Curry, 2001: Simulation of arctic low-level clouds observed during the FIRE Arctic Clouds Experiment using a new bulk microphysics scheme. Journal of Geophysical Research: Atmospheres (1984–2012), 106, 15139-15154.

Gunn, R., and B. Phillips, 1957: An experimental investigation of the effect of air pollution on the initiation of rain. Journal of Meteorology, 14, 272-280.

Harrington, J. Y., M. P. Meyers, R. L. Walko, and W. R. Cotton, 1995: Parameterization of ice crystal conversion processes due to vapor deposition for mesoscale models using double-moment basis functions. Part I: Basic formulation and parcel model results. Journal of the Atmospheric Sciences, 52, 4344-4366.

Hobbs, P. V., L. F. Radke, and S. E. Shumway, 1970: Cloud Condensation Nuclei from Industrial Sources and Their Apparent Influence on Precipitation in Washington State. Journal of the Atmospheric Sciences, 27, 81-89.

Khain, A., 2009: Notes on state-of-the-art investigations of aerosol effects on precipitation: a critical review. Environmental Research Letters, 4, 015004.

Khain, A., A. Pokrovsky, M. Pinsky, A. Seifert, and V. Phillips, 2004: Simulation of effects of atmospheric aerosols on deep turbulent convective clouds using a spectral microphysics mixed-phase cumulus cloud model. Part I: Model description and possible applications. Journal of the Atmospheric Sciences, 61, 2963-2982.

Khain, A., and G. Sutyrin, 1983: Tropical Cyclones and their Interaction with the Ocean. Gidrometeoizdat, Leningrad, 241.

Khain, A., D. Rosenfeld, and A. Pokrovsky, 2005: Aerosol impact on the dynamics and microphysics of deep convective clouds. Quarterly Journal of the Royal Meteorological Society, 131, 2639-2663.

Khain, A., L. Leung, B. Lynn, and S. Ghan, 2009: Effects of aerosols on the dynamics and microphysics of squall lines simulated by spectral bin and bulk parameterization schemes. Journal of Geophysical Research: Atmospheres (1984–2012), 114.

Lin, Y.-L., R. D. Farley, and H. D. Orville, 1983: Bulk parameterization of the snow field in a cloud model. Journal of Climate and Applied Meteorology, 22, 1065-1092.

Lohmann, U., 2002: A glaciation indirect aerosol effect caused by soot aerosols. Geophysical Research Letters, 29, 1052.

Martin, G., D. Johnson, and A. Spice, 1994: The measurement and parameterization of effective radius of droplets in warm stratocumulus clouds. Journal of the Atmospheric Sciences, 51, 1823-1842.

Morrison, H., and J. Pinto, 2005: Mesoscale modeling of springtime Arctic mixed-phase strati-form clouds using a new two-moment bulk microphysics scheme. Journal of the Atmospheric Sciences, 62, 3683-3704.

Morrison, H., J. Curry, and V. Khvorostyanov, 2005: A new double-moment microphysics parameterization for application in cloud and climate models. Part I: Description. Journal of the Atmospheric Sciences, 62, 1665-1677.

Penner J.E., e. a.: Aerosols, their Direct and Indirect Effects. Assessment, 5, 289- 348.

Ramanathan, V., P. Crutzen, J. Kiehl, and D. Rosenfeld, 2001: Aerosols, climate, and the hydrological cycle. Science, 294, 2119-2124.

Reisner, J., R. Rasmussen, and R. Bruintjes, 1998: Explicit forecasting of super cooled liquid water in winter storms using the MM5 mesoscale model. Quarterly Journal of the Royal Meteorological Society, 124, 1071-1107.

Rosenfeld, D., 1999: TRMM observed first direct evidence of smoke from forest fires inhibiting rainfall. Geophysical Research Letters, 26, 3105-3108.

Rosenfeld, D., 2000: Suppression of rain and snow by urban and industrial air pollution. Science, 287, 1793-1796.

Rosenfeld, D., A. Khain, B. Lynn, and W. Woodley, 2007: Simulation of hurricane response to suppression of warm rain by sub-micron aerosols. Atmospheric Chemistry and Physics, 7, 3411-3424.

Rosenfeld, D., and A. Khain, 2008: Anthropogenic aerosol invigorating hail. Preprints, Proc. Int. Conf. on Clouds and Precipitation (Cancun, July 2008).

Rosenfeld, D., et al., 2008: Flood or drought: how do aerosols affect precipitation? Science, 321, 1309-1313.

Rutledge, S. A., and P. V. Hobbs, 1984: The mesoscale and microscale structure and organization of clouds and precipitation in midlatitude cyclones. XII: A diagnostic modeling study of precipitation development in narrow cold-frontal rain bands. Journal of Atmospheric Sciences, 41, 2949-2972.

Simpson, R., and J. S. Malkus, 1964: Experiments in hurricane modification. Scientific American, 211, 27-37.

Takeda, T., and N. Kuba, 1982: Numerical study of the effect of CCN on the size distribution of cloud droplets. I- Cloud droplets in the stage of condensation growth (Cloud Condensation Nuclei). Meteorological Society of Japan, Journal, 60, 978-993.

Twomey, S., 1974: Pollution and the planetary albedo. Atmospheric Environment (1967), 8, 1251-1256.

Twomey, S., 1977: The influence of pollution on the shortwave albedo of clouds. Journal of Atmospheric Sciences, 34, 1149-1152.

Vaid, B. H. 2013: Numerical Simulations and analysis of heavy rainfall event over Singapore using the WRFV3 Model. International Journal of Atmospheric Sciences, Article ID 825395, 8 pages. doi:10.1155/2013/825395.

Walko, R. L., W. R. Cotton, M. Meyers, and J. Harrington, 1995: New RAMS cloud microphysics parameterization Part I: the single-moment scheme. Atmospheric Research, 38, 29-62.

Zhang, H., G. M. McFarquhar, S. M. Saleeby, and W. R. Cotton, 2007: Impacts of Saharan dust as CCN on the evolution of an idealized tropical cyclone. Geophysical Research Letters, 34.

Zhang, R., et al., 2004: Atmospheric new particle formation enhanced by organic acids. Sciences, 304, 1487-1490.